Ultrafast Photophysical Investigation of Cresyl Violet Aggregates Adsorbed onto Nanometer-Sized Particles of SnO_2 and SiO_2

Ignacio Martini and Gregory V. Hartland*

Department of Chemistry and Biochemistry, University of Notre Dame, Notre Dame, Indiana 46556

Prashant V. Kamat

Radiation Laboratory, University of Notre Dame, Notre Dame, Indiana 46556

Received: January 23, 1997; In Final Form: March 17, 1997[⊗]

The relaxation dynamics of cresyl violet H-aggregate dimers adsorbed onto SnO_2 or SiO_2 colloidal particles has been examined with ca. 200 fs time resolution. These experiments were performed by monitoring both the ground state recovery of the excited dye molecules and the transient absorption signal in the region of the dye radical cation. For cresyl violet−SiO_2, the ground state recovery is a single exponential with a 2.9 ± 0.2 ps time constant. Transient absorption measurements that monitored the excited electronic state of the dye show a similar 2.5 ± 0.4 ps decay. The observed dynamics for cresyl violet−SiO_2 is assigned to internal conversion followed by vibrational relaxation of the adsorbed cresyl violet dimers. The similarity of the transient absorption and bleach recovery time constants shows that vibrational relaxation is extremely rapid, i.e., internal conversion is the rate-limiting step. For cresyl violet−SnO_2, the ground state recovery is biexponential with time constants of 2.4 ± 0.4 ps (∼80% of the amplitude) and 11.3 ± 0.5 ps (∼20%). Transient absorption measurements that monitor both the electronically excited dye aggregates and the dye radical cation also show a biexponential decay with time constants of 2.3 ± 0.3 and 12.3 ± 0.5 ps. The 2.4 ps process is attributed to internal conversion/vibrational relaxation of the excited dye aggregates, analogous to the results for the cresyl violet-SiO_2 system. The 12 ps process is assigned to the decay of the cresyl violet dimer radical cation that is produced by electron transfer to the SnO_2 semiconductor particles. The radical cation only contributes to the signal for the cresyl violet−SnO_2 system because electron transfer to SiO_2 is not energetically allowed. The decay mechanism for the radical cation is back electron transfer from SnO_2.

Introduction

Dye sensitization of wide band gap semiconductor particles is important in a variety of applications, including photography,[1] solar energy conversion,[2,3] and photocatalytic waste water remediation.[4,5] In all of these examples the primary event is the creation of a charge separation by electron transfer from the photoexcited dye to the semiconductor. The efficiency of charge separation depends on the relative magnitude of the electron transfer rate constant (k_{et}) to the rate of back electron transfer (k_b) and nonradiative decay (k_{nr}) of the adsorbed dye molecules. However, despite the importance of dye sensitization, very few ultrafast laser studies of the photophysics of dye molecules adsorbed at semiconductor particle surfaces have been reported to date.[6,7] Thus, not much is known about how k_{et}, k_b, and k_{nr} vary for different dye semiconductor particle systems and what the important factors are in determining the magnitude of these rate constants.

In this paper ultrafast transient absorption/bleach recovery data for cresyl violet (CV^+) adsorbed onto nanometer-sized particles of SnO_2 and SiO_2 is presented. These experiments were performed by employing a home-built optical parametric amplifier (OPA) for the pump laser source.[8,9] The OPA can supply 200−250 fs pump laser pulses with wavelengths anywhere from 750 to 450 nm. This tunability is a key factor for the success of our experiments; it allows us to selectively excite the adsorbed dye molecules and not the semiconductor, so that the ultrafast dynamics of the dye can be unambiguously measured. SnO_2 and SiO_2 particles were chosen for study because electron transfer from cresyl violet is energetically allowed to SnO_2 but not to SiO_2.[10] Thus, comparing the experimental results for these two systems provides a way of unraveling electron transfer from other photophysical processes.

Previous experiments have determined that cresyl violet forms dimers ($(CV^+)_2$) on the surface of SnO_2 or SiO_2 particles and that the $(CV^+)_2$ absorbance spectrum is blue shifted by ca. 65 nm compared to the monomer.[10] This shows that $(CV^+)_2$ has a "H-aggregate" geometry, i.e., the transition dipole moments of the cresyl violet molecules in the dimer are parallel to each other.[11] In this geometry optical transitions from the S_0 state are only allowed to the upper S_1^+ component of the pair of excited singlet states produced by exciton coupling.[11] Note that fluorescence cannot be observed from $(CV^+)_2$, for either dimers adsorbed onto semiconductor particles[10] or for free dimers in solution.[12] This is a general property of H-aggregates that is attributed to fast internal conversion (IC) from the optically excited S_1^+ state to the lower S_1^- component of the exciton pair of states.[11] This process quenches fluorescence because optical transitions from the S_1^- state to the ground S_0 electronic state are forbidden.[11] In solution phase, H-aggregates in the S_1^- state are deactivated by either intersystem crossing (ISC) to the triplet T_1 state or by a second IC process to the S_0 state. Note that the ISC channel is often enhanced in H-aggregates because the S_1^-−T_1 energy gap is reduced by the exciton splitting of the S_1 state.[11]

For $(CV^+)_2$ adsorbed onto semiconductor particles, electron transfer from the dye to the semiconductor is also possible. Transient absorption experiments recorded with ∼20 ps time

* Author to whom correspondence should be addressed: E-mail: hartland.1@nd.edu.

[⊗] Abstract published in *Advance ACS Abstracts,* June 1, 1997.

S1089-5647(97)00296-4 CCC: $14.00

resolution, which monitored the $(CV^+)_2^{\bullet+}$ radical cation, show that electron transfer to SnO_2 occurs from the triplet state of the dimer on a slow 5 ns time scale. Photoelectrochemical and time-resolved microwave absorption studies of thin films constructed from $(CV^+)_2-SnO_2$ particles have also shown that the photon-to-photocurrent efficiency is low, ~1%.[13] Note that the S_1^+ state of the cresyl violet dimer is ~1.4 eV higher in energy than the conduction band of SnO_2, whereas the S_1^- state is ~0.8 eV higher.[2,14] Thus, the electron transfer rates from the S_1^- and S_1^+ states of cresyl violet to SnO_2 may be different. The aim of this paper is to determine why the photon-to-photocurrent conversion efficiency is so low for this system, i.e., what processes control the photophysics of cresyl violet adsorbed onto semiconductor particle surfaces.

Experimental Section

Aqueous colloidal suspensions of SnO_2 (18%, Alfa Chemicals) and SiO_2 (14.5%, NALCO Chemical Company) were used as received. The diameter of the particles was measured by TEM (380 000× magnification) to be 30−50 Å for both SiO_2 and SnO_2. Cresyl violet was obtained from Exciton and was used without further purification. Samples were prepared by diluting the stock colloid solutions to a particle concentration of 5 μM and adding concentrated dye solution. The final dye concentration was ca. 40 μM. All experiments were performed in distilled water. Due to strong electrostatic interactions between the cationic dye and the negatively charged particles, the cresyl violet molecules are almost completely adsorbed onto the particle surface. For both systems, cresyl violet exists as dimers on the surface, even at low dye concentrations.[10] In the experiments reported below, there were approximately 4−5 cresyl violet dimers/particle, which implies an average distance of 40−50 Å between dimers. Note that, at the dye/particle concentrations used in our study, only ca. 1% of the CV^+ molecules exist as free monomers in solution.

The laser system used for these experiments is based on a mode-locked Ti:Sapphire laser (Clark-MXR, NJA-4) that is pumped by a Coherent I-90/6 argon ion laser. The beam from the oscillator (0.4 W, 50−60 fs fwhm) is regeneratively amplified (Clark-MXR, CPA-1000) to yield pulses with >0.5 mJ energy at a 1 kHz repetition rate and with typical pulsewidths of 120 fs ($sech^2$ deconvolution). The output from the regenerative amplifier is split by a 90−10 beam splitter, and the 90% portion pumps the OPA. The OPA produces tunable pump laser pulses, with microjoule energies per pulse. The design is based on that of Greenfield et al.[8] and is described in detail in ref 9. The 10% portion of the beam from the regenerative amplifier supplies the probe laser pulses. Tunable visible probe pulses are obtained by attenuating the 10% beam with a variable neutral density filter (Edmund Scientific) and focusing into a 6 mm BK-7 window to produce a white light continuum. Band-pass interference filters (10 nm, Oriel) were used to select slices from the continuum. Probe laser pulses with $\lambda = 400$ nm were obtained by doubling the 10% beam in a 300 μm KDP crystal.

The pump and probe beams were cross overlapped at the sample by focusing with a 10 cm lens. The sample solution was flowed through a 3 mm path length cell that was placed slightly before the focus of the pump and probe lasers (we have found that this significantly reduces unwanted nonlinear effects in the signal). The transmitted intensity of the probe was detected with an amplified Si-PIN photodiode (Thorlabs, PA150), and the signal was normalized using the scheme described in ref 15. Briefly, the probe is divided into signal and reference beams before the sample, and the intensities of these beams are converted to quasi-dc voltages by gated integration of the photodiode signal. An inexpensive analog division integrated circuit (Burr Brown, DIV100) generates a normalized signal, which is fed into a lock-in amplifier (Stanford Instruments, SR830). The lock-in is referenced to a chopper that modulates the pump laser. This scheme efficiently normalizes fluctuations in the probe laser on a pulse-to-pulse basis.[15] Typically, the absorbance change induced by the pump laser in the dye−semiconductor systems was 2−3 mo.d.

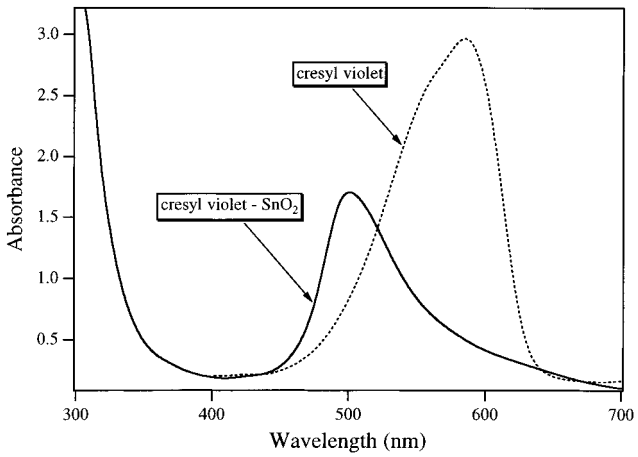

Figure 1. Steady state UV−vis absorption spectra of (a) 40 μM cresyl violet monomer and (b) 42 μM cresyl violet and 5 μM SnO_2 particle concentration. Both spectra were recorded in aqueous solution.

The delay between the pump and probe pulses was varied with a 0.1 μm resolution stepper-motor driven translation stage (Newport, UTM150PP.1). Data collection and the movement of the translation stage were controlled by a LabVIEW program that runs on a Power Macintosh 7100/80 personal computer. Data analysis was performed by a deconvolution and fitting routine that uses the Levenberg−Marquardt nonlinear least-squares method.[16] The instrument response function was assumed to be a Gaussian with a fwhm determined from the cross correlation between the 780 nm fundamental and the OPA. The cross-correlations were measured with a 300 μm KDP crystal, and typical values for the fwhm were 220−280 fs (Gaussian deconvolution).

Results

UV−vis absorption spectra of CV^+ in aqueous solution and of $(CV^+)_2$ adsorbed onto the surface of SnO_2 particles are presented in Figure 1. The spectrum for $(CV^+)_2-SiO_2$ is very similar to that shown for $(CV^+)_2-SnO_2$, except that the UV absorption ($\lambda < 350$ nm) due to the SnO_2 particles is absent. In Figure 2 transient bleach/stimulated emission data for the cresyl violet monomer is presented. These experiments were performed with 500 nm pump and 550 nm probe laser pulses. The signal shows an initial 0.87 ± 0.05 ps decay (~60% of the amplitude) due to vibrational relaxation and/or solvation effects, followed by a much slower decay that is consistent with the 2.2 ns fluorescence lifetime of aqueous cresyl violet.[12]

Figure 3 shows transient bleach data for $(CV^+)_2-SnO_2$ and $(CV^+)_2-SiO_2$. These experiments were performed with 500 nm pump laser pulses and a probe laser wavelength of 530 nm. These pump and probe wavelengths correspond to the maxima of the steady-state absorption and transient bleach spectra, respectively, for $(CV^+)_2-SnO_2$.[10] In addition, the contribution from free CV^+ monomer to the signal is minimized at 530 nm, because the signal from CV^+ changes from a transient absorption to a transient bleach near this wavelength.[10] Clearly, the time response of the transient bleach signal for the dye−semiconductor particle systems is very different to that for the

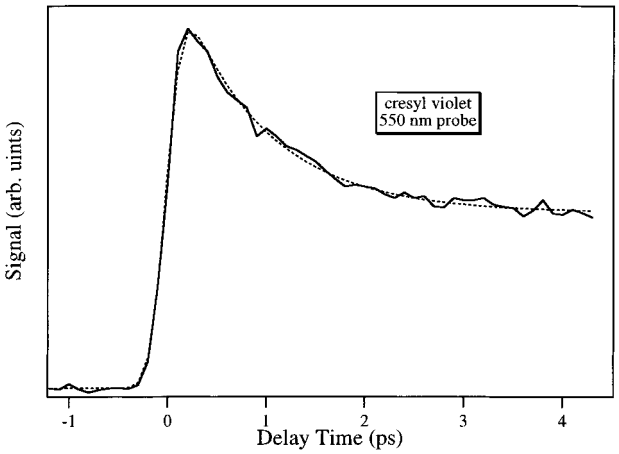

Figure 2. Transient bleach/stimulated emission data recorded with 500 nm pump and 550 nm probe pulses for the cresyl violet monomer in aqueous solution: (—) experimental data, (···) theoretical fit to the data.

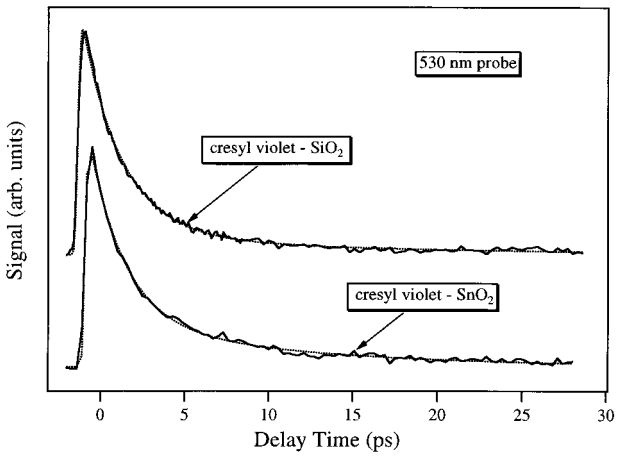

Figure 3. Transient bleach data recorded with 500 nm pump and 530 nm probe pulses for cresyl violet dimers adsorbed onto the surface of SnO_2 and SiO_2 particles: (—) experimental data, (···) theoretical fit to the data.

cresyl violet monomer. Specifically, the bleach recovery is almost complete within 20 ps for both $(CV^+)_2-SnO_2$ and $(CV^+)_2-SiO_2$. Also shown in Figure 3 is a fit to the experimental data. This analysis shows that for $(CV^+)_2-SiO_2$ the transient bleach signal has a single exponential decay with a 2.9 ± 0.2 ps time constant. In contrast, for $(CV^+)_2-SnO_2$, the decay is biexponential with time constants of 2.4 ± 0.4 and 11.3 ± 0.5 ps that account for 80% and 20% of the signal amplitude, respectively.

Figures 4 and 5 show transient absorption data collected with 500 nm pump laser pulses and a probe laser wavelength of 400 nm. The results for the CV^+ monomer are shown in Figure 4 and data for $(CV^+)_2-SnO_2$ and $(CV^+)_2-SiO_2$ are shown in Figure 5. The λ = 400 nm probe laser pulses interrogate electronically excited $CV^+/(CV^+)_2$,[10] as well as the $CV^{\bullet 2+}/(CV^+)_2^{\bullet +}$ radical cations.[17] Note that both the S_1^+ and S_1^- states of $(CV^+)_2$ can give rise an absorption signal in this experiment. Similar to the data shown in Figure 2, the transient absorption signal for the CV^+ monomer shows a fast decay component (1.0 ± 0.1 ps, 45% of the amplitude) followed by a slower decay that is consistent with the 2.2 ns monomer fluorescence lifetime. Again, the fast decay is most likely due to vibrational relaxation and/or solvation dynamics in the S_1 state of CV^+. At early times (<20 ps) the transient absorption signals for $(CV^+)_2-SnO_2$ and $(CV^+)_2-SiO_2$ show a similar time behavior to the data presented in Figure 3. However, instead of decaying to zero at long times, the transient absorption signal for $(CV^+)_2-SnO_2$ and $(CV^+)_2-SiO_2$ reaches a constant level of ~10% of the maximum. This long time contribution to the signal is due to free CV^+ monomer in solution and/or triplet $(CV^+)_2$ species produced by intersystem crossing from the S_1^- state.

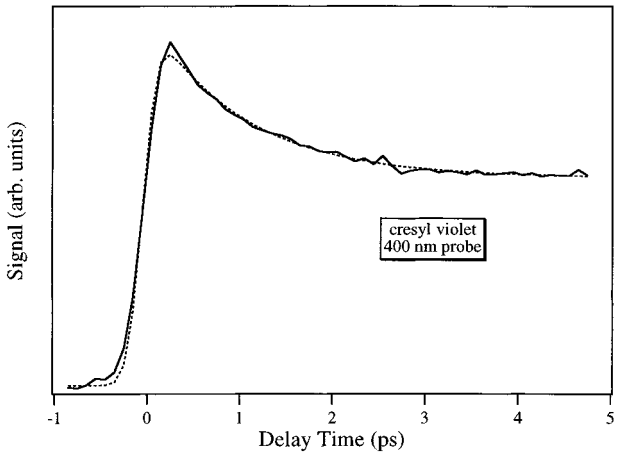

Figure 4. Transient absorption data recorded with 500 nm pump and 400 nm probe laser pulses for the cresyl violet monomer in aqueous solution: (—) experimental data, (···) theoretical fit to the data.

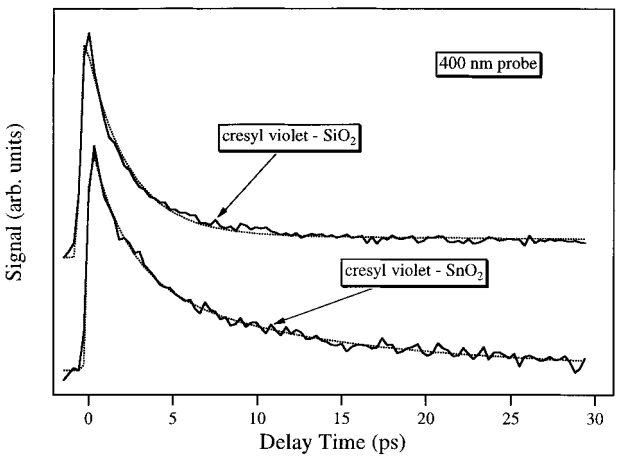

Figure 5. Transient absorption data recorded with 500 nm pump and 400 nm probe pulses for cresyl violet dimers adsorbed onto the surface of SnO_2 and SiO_2 particles: (—) experimental data, (···) theoretical fit to the data.

Fits to the data using an offset plus a single exponential for $(CV^+)_2-SiO_2$ and a double exponential for $(CV^+)_2-SnO_2$ are shown in Figure 5. Note that the 1 ps decay observed for the CV^+ monomer in Figure 4 should also contribute to the data shown in Figure 5. However, because the amplitude of this signal is within the signal-to-noise of the experiment, this decay component was not included in the data analysis. The parameters obtained from these fits are not as reliable as those from the transient bleach data in Figure 3, due to the lower signal-to-noise ratio for the 400 nm probe data and the contribution from the CV^+ monomer/$(CV^+)_2$ triplet to the signal. For $(CV^+)_2-SiO_2$ our analysis yields a decay time 2.5 ± 0.4 ps. For $(CV^+)_2-SnO_2$, the decay time constants obtained are 2.3 ± 0.3 and 12.3 ± 0.5 ps, with relative amplitudes of 3:2. Note that for both probe wavelengths the dynamics observed for $(CV^+)_2-SnO_2$ is slower than that for $(CV^+)_2-SiO_2$. Also, for a given system, the time constants determined from the bleach recovery data (Figures 3) and the transient absorption measurements (Figure 5) are within experimental error.

Discussion

The results presented in Figures 3 and 5 can be explained using the energy level diagram shown in Figure 6. Specifically,

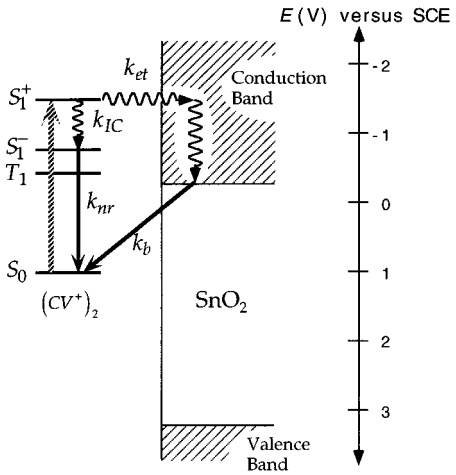

Figure 6. Energy level diagram for electron transfer and nonradiative relaxation in $(CV^+)_2$-SnO_2. S_1^+ and S_1^- are the excited singlet states created by exciton splitting in the dimer; T_1 is the triplet state; S_0 is the ground electronic state; and k_{et}, k_{IC}, k_{nr}, and k_b are the rate constants for electron transfer, $S_1^+ \rightarrow S_1^-$ IC, and nonradiative decays of the S_1^- state and back electron transfer, respectively.

the pump laser excites levels in the S_1^+ state of $(CV^+)_2$, and these levels subsequently undergo IC to the S_1^- state.[11] Anfinrud and co-workers were unable to detect fluorescence from $(CV^+)_2$ in solution,[12] which implies that the quantum yield for $S_1^+ \rightarrow S_1^-$ IC is ≈1. The $S_1^+ \rightarrow S_1^-$ IC process (which is a property of the dimer and is not induced by interactions with the colloid particles) also completely quenches the $(CV^+)_2$ fluorescence in the $(CV^+)_2-SnO_2$ and $(CV^+)_2-SiO_2$ systems.[10] We believe that $S_1^+ \rightarrow S_1^-$ IC is extremely fast (<100 fs), so that the S_1^+ state does not significantly contribute to either the 530 nm probe experiments (through stimulated emission) or the 400 nm transient absorption experiments, for both $(CV^+)_2-SnO_2$ and $(CV^+)_2-SiO_2$.[18] Unfortunately, we were unable to produce cresyl violet dimers in solution without also producing larger dye aggregates. Thus, we could not examine the dynamics of $(CV^+)_2$ without the presence of SiO_2 or SnO_2 particles.

For $(CV^+)_2-SnO_2$, electron transfer to the SnO_2 particles also occurs from the S_1^+ state and, therefore, competes with the $S_1^+ \rightarrow S_1^-$ IC process, see Figure 6. The relative number of species that undergo $S_1^+ \rightarrow S_1^-$ IC compared to electron transfer is determined by the relative magnitudes of the internal conversion and electron transfer rate constants, k_{IC}/k_{et}. The electron transfer process generates the $(CV^+)_2^{\bullet+}$ radical cation, which is destroyed by back electron transfer from the SnO_2 particle−regenerating ground state $(CV^+)_2$. The S_1^- levels produced by the $S_1^+ \rightarrow S_1^-$ IC process decay by a second $S_1^- \rightarrow S_0$ IC step, with a small number of species undergoing ISC to the T_1 state. The highly vibrationally excited S_0 molecules produced by $S_1^- \rightarrow S_0$ IC are subsequently vibrationally deactivated. In this scheme the 400 nm transient absorption measurements, which probe both $(CV^+)_2^{\bullet+}$ and electronically excited $(CV^+)_2$, should show two components: a growth and decay due to the formation and disappearance of the $(CV^+)_2^{\bullet+}$ radical cation and a second decay due to $S_1^- \rightarrow S_0$ IC. In turn, the 530 nm bleach recovery experiments should also show two components due to the two pathways for repopulating the $(CV^+)_2$ ground state (decay of the $(CV^+)_2^{\bullet+}$ radical cation and $S_1^- \rightarrow S_0$ IC followed by vibrational relaxation). Our data is consistent with this picture: both the transient absorption and bleach recovery data for $(CV^+)_2-SnO_2$ show biexponential decays with time constants of 2.4 and ca. 12 ps. We do not observe a growth in the 400 nm transient absorption signal due to the formation of the $(CV^+)_2^{\bullet+}$ radical cation. This is not surprising as electron transfer is expected to be extremely fast (∼ 200 fs, vide infra). In addition, because the S_1^+ and S_1^- states of $(CV^+)_2$ and the $(CV^+)_2^{\bullet+}$ radical cation all absorb at 400 nm, the growth in the 400 nm transient absorption signal due to the formation of $(CV^+)_2^{\bullet+}$ will be masked by the decay of the electronically excited $(CV^+)_2$ species. Note that without further information it is difficult to determine whether the 2.4 ps time constant is due to $S_1^- \rightarrow S_0$ IC and the 12 ps time constant is due to back electron transfer or visa versa.

On the other hand, for $(CV^+)_2-SiO_2$ electron transfer to the colloid particle cannot occur: the pump laser excited $(CV^+)_2$ species can only return to the ground state via $S_1^- \rightarrow S_0$ IC. Thus, the 400 nm transient absorption signal should show a single exponential decay due to $S_1^- \rightarrow S_0$ IC. Likewise, the bleach recovery measurements should show a single exponential with a time constant determined by the rate of $S_1^- \rightarrow S_0$ IC convoluted with the rate of vibrational deactivation. Again, this prediction is consistent with our data. Note that the time constants for the decay of the S_1^- excited state absorption at 400 nm (2.5 ± 0.4 ps) and that the bleach recovery at 530 nm (2.9 ± 0.2 ps) are within experimental error. This implies that vibrational relaxation in the ground electronic state of $(CV^+)_2-SiO_2$ is extremely fast, i.e., $S_1^- \rightarrow S_0$ IC is the rate-limiting step. This is also true for $(CV^+)_2-SnO_2$, the bleach recovery time constants (2.4 ± 0.4 and 11.3 ± 0.5 ps) are within experimental error of the transient absorption decays (2.3 ± 0.3 and 12.3 ± 0.5 ps), indicating that vibrational relaxation is extremely fast.

By comparison to the results for $(CV^+)_2-SiO_2$, the 2.4 ps time constant observed in the transient absorption data for $(CV^+)_2-SnO_2$ is assigned to $S_1^- \rightarrow S_0$ IC. This assignment is based on the fact that this time constant is very close to the 2.5 ps time constant observed for $(CV^+)_2-SiO_2$. Thus, the 12 ps decay in the $(CV^+)_2-SnO_2$ transient absorption and bleach recovery experiments is assigned to the decay of the $(CV^+)_2^{\bullet+}$ radical cation through back electron transfer from SnO_2. A time scale of 12 ps for the back electron transfer reaction is in agreement with recent measurements for dye molecules adsorbed onto the surface of bulk semiconductors.[19]

The relative amplitude of the two exponentials in the $(CV^+)_2-SnO_2$ bleach recovery data is determined by the relative yields of the IC and electron-transfer pathways. Specifically, the data in Figure 3 shows that for $(CV^+)_2-SnO_2$ the number of species that undergo IC compared to electron transfer is ca. 4:1. Thus, the ratio of the $S_1^+ \rightarrow S_1^-$ IC and electron transfer rate constants is $k_{IC}/k_{et} = 4 \pm 1$. Previous ultrafast studies of dye−semiconductor particle systems have determined electron transfer times of ca. 200 fs.[6,7] Using this number as the time constant for electron transfer in $(CV^+)_2-SnO_2$ implies that the time scale for $S_1^+ \rightarrow S_1^-$ IC must be ca. 40−70 fs. This time scale is consistent with our data: $S_1^+ \rightarrow S_1^-$ IC is much faster than our time resolution and would not be observed in the transient absorption measurements presented in Figure 5. Note that in our system the dye molecules are electrostatically attached to the surface, whereas in refs 6 and 7, the dye molecules were covalently bonded. Thus, the electronic couplings may be different, and the time scale of 200 fs determined in refs 6 and 7 only provides a rough estimate of the electron transfer time for $(CV^+)_2-SnO_2$.

Picosecond transient absorption measurements have shown that a small fraction of the excited dimers end up in the T_1 state and that the lifetime of the T_1 state is much greater than 20 ps.[10] Thus, the almost complete bleach recoveries observed for $(CV^+)_2-SiO_2$ and $(CV^+)_2-SnO_2$ in Figure 3 indicate that

the quantum yield for ISC is <3% for these systems (this limit is established by the signal-to-noise in the data, see Figure 3). For $(CV^+)_2-SnO_2$, the species that end up in the triplet state undergo electron transfer to SnO_2 on a 5 ns time scale, giving rise to photo-conductivity in $(CV^+)_2-SnO_2$ particle films.[13] The low quantum yield of triplet $(CV^+)_2$ determined from our measurements is one reason for the low photon-to-photocurrent conversion efficiency measured of these films.[13] In addition, nanosecond transient absorption and time-resolved microwave conductivity measurements of the $(CV^+)_2-SnO_2$ particle films show that the charge separation created by electron transfer from the T_1 state decays with a rate constant of 9×10^6 s^{-1} at low pump laser power and that this decay rate increases to 20×10^6 s^{-1} when the laser power is increased by a factor of 4.[13] These results imply that electron transfer from the triplet state of $(CV^+)_2$ occurs to trap sites at the SnO_2 particle surface and that the mechanism for charge recombination is detrapping followed by fast back electron transfer. Specifically, increasing the laser power produces more electrons which fill up the lower energy trap sites. Thus, higher energy trap sites that have faster detrapping times are populated at high laser power, leading to an increase in the observed recombination rate.[13] This mechanism, where detrapping is the rate limiting step, is consistent with the fast 12 ps back electron transfer time constant measured in this work.

Several other mechanisms have been considered to explain our experimental data: first, electron transfer could occur from the S_1^- state rather than the S_1^+ state. However, the ratio of the two exponentials in the bleach recovery measurements implies that the time scale for electron transfer in this case should be a ca. 10 ps (given that the time scale for $S_1^- \rightarrow S_0$ IC is 2.5 ps and $k_{IC}/k_{et} = 4$). This would lead to complicated kinetics in the transient absorption and bleach recovery data, which is not consistent with our observations of simple double-exponential decays for $(CV^+)_2-SnO_2$. A second possibility is that both electron transfer to SnO_2 and IC to the S_0 state occur directly from the S_1^+ state. In this case the 2 ps process must be assigned to IC between the S_1^+ and S_0 states. Again, the ratio of the amplitudes in the transient bleach data implies an electron transfer time of ~10 ps, which is not observed in the data shown in Figures 3 and 5.

A final possible explanation for the SnO_2 data shown in Figures 3 and 5 is that there are multiple sites for $(CV^+)_2$ adsorption at the surface of the SnO_2 particles, but not for SiO_2. Specifically, for SnO_2, one site gives a 2.4 ps relaxation time and the other yields a 12 ps relaxation time, and there is no electron transfer. However, the different adsorption sites should have different $S_1^+ \leftarrow S_0$ transition frequencies. Thus, the transient bleach data should change as the pump laser wavelength is changed. Experiments performed with different pump wavelengths yield similar results to those shown in Figure 3. Furthermore, if this mechanism were correct the relative amplitudes of the 2.4 and 12 ps time constant exponentials observed for $(CV^+)_2-SnO_2$ should be the same for the 400 and 530 nm probe experiments. This is clearly not the case. Thus, the biexponential decay observed for $(CV^+)_2$-SnO_2 is not due to a heterogeneous distribution of adsorption sites. The most likely explanation for the results presented in Figures 3 and 5 is that electron transfer to SnO_2 occurs from the S_1^+ state of $(CV^+)_2$ in competition with $S_1^+ \rightarrow S_1^-$ IC and that the 2−3 ps process observed for both SiO_2 and SnO_2 is IC from the S_1^- state to the S_0 state.

Summary and Conclusions

The photoconversion efficiency in dye-sensitized semiconductor particles depends on the rate of electron transfer relative to the rate of nonradiative decay of the dye and the rate of back electron transfer from the semiconductor to the dye. In this paper we have examined the ultrafast dynamics of cresyl violet dimers adsorbed onto the surface of SnO_2 and SiO_2 particles by both transient absorption and bleach recovery experiments. These measurements show that (1) Nonradiative relaxation of the photoexcited cresyl violet dimers occurs by consecutive internal conversion steps. Specifically, the optically excited S_1^+ species undergo rapid $S_1^+ \rightarrow S_1^-$ IC, followed by a slower $S_1^- \rightarrow S_0$ IC process that occurs on a 2−3 ps time scale. The highly vibrationally excited S_0 state species produced are rapidly deactivated, leading to ground state recovery times of 2.4 ± 0.4 ps for $(CV^+)_2-SnO_2$ and 2.9 ± 0.2 ps for $(CV^+)_2-SiO_2$. (2) For $(CV^+)_2-SnO_2$, approximately 20% of the excited S_1^+ dimers transfer an electron to the SnO_2 particle. The subsequent back electron transfer reaction occurs with a 12 ps time constant.

Acknowledgment. Acknowledgment is made to the donors of The Petroleum Research Fund, administered by the American Chemical Society, and the University of Notre Dame Faculty Research Program for support of this research. The authors would also like to thank Di Liu for helpful suggestions on various aspects of this work. P.V.K. was supported by the office of Basic Energy Science of the U.S. Department of Energy. This is contribution 3967 from the Notre Dame Radiation Laboratory.

References and Notes

(1) Bourdon, J. *J. Phys. Chem.* **1965**, *69*, 705.

(2) Hagfeldt, A.; Grätzel, M. *Chem. Rev.* **1995**, *95*, 49.

(3) Henglein, A. *Chem. Rev.* **1989**, *89*, 1861.

(4) Kamat, P. V. *Chem. Rev.* **1993**, *93*, 267.

(5) Hoffmann, M. R.; Martin, S. T.; Choi, W.; Bahnemann, D. W. *Chem. Rev.* **1995**, *95*, 69.

(6) (a) Moser, J. E.; Gratzel, M.; Durrant, J. R.; Klug, D. R. In *Femtochemistry: Ultrafast Chemical and Physical Processes in Molecular Systems*; Chergui, M., Ed.; World Scientific: Singapore, 1996. (b) Rehm, J. M.; McLendon, G. L.; Nagasawa, Y.; Yoshihara, K.; Moser, J.; Grätzel, M. *J. Phys. Chem.* **1996**, *100*, 9577.

(7) Burfeindt, B.; Hannappel, T.; Storck, W.; Willig, F. *J. Phys. Chem.* **1996**, *100*, 16463.

(8) (a) Greenfield, S. R.; Wasielewski, M. R. *Appl. Opt.* **1995**, *34*, 2689. (b) Greenfield, S. R.; Wasielewski, M. R. *Opt. Lett.* **1995**, *20*, 1395.

(9) Martini, I.; Hartland, G. V. *Chem. Phys. Lett.* **1996**, *258*, 180.

(10) Liu, D.; Kamat, P. V. *J. Chem. Phys.* **1996**, *105*, 965.

(11) McRae, E. G.; Kasha, M. The Molecular Exciton Model. In *Physical Processes in Radiation Biology*; Augenstein, L., Mason, R., Rosenberg, B., Eds.; Academic Press: New York, 1964.

(12) Anfinrud, P.; Crackel, R. L.; Struve, W. S. *J. Phys. Chem.* **1984**, *88*, 5873.

(13) Liu, D.; Fessenden, R. W.; Hug, G. L.; Kamat, P. V. *J. Phys. Chem.* **1997**, *101*, 2583.

(14) Parkinson, B. A. *Langmuir* **1988**, *4*, 967.

(15) Martini, I.; Hodak, J.; Hartland, G. V., in preparation.

(16) Press, W. H.; Teukolsky, S. A.; Vetterling, W. T.; Flannery, B. P. *Numerical Recipes*, 2nd ed.; Cambridge University Press: Cambridge, 1992.

(17) Kreller, D. I.; Kamat, P. V. *J. Phys. Chem.* **1991**, *95*, 4406.

(18) Note that because both the S_1^- and S_1^+ states can contribute to the transient absorption signal at 400 nm, the decay of the S_1^+ state signal would be masked by the growth in the S_1^- signal, making it difficult to observe the $S_1^+ \rightarrow S_1^-$ IC process by transient absorption.

(19) Lanzafame, J. M.; Palese, S.; Wang, D.; Miller, R. J. D.; Muenter, A. A. *J. Phys. Chem.* **1994**, *98*, 11020.